Biophysical Journal

Supporting Material

The Phylogenetic Signature Underlying ATP Synthase c-ring Compliance

Alessandro Pandini,[1] Jens Kleinjung,[2] Willie R. Taylor,[2] Wolfgang Junge,[3] and Shahid Khan[2,4,*]

[1]Department of Computer Science and Synthetic Biology Theme, Brunel University London, Uxbridge, United Kingdom; [2]Mathematical Biology, The Francis Crick Institute (formerly the National Institute for Medical Research), London, United Kingdom; [3]Department of Biophysics, University of Osnabrück, Osnabrück, Germany; and [4]Molecular Biology Consortium, Lawrence Berkeley National Laboratory, Berkeley, California

SUPPLEMENTARY MATERIAL

Figure S1: GSATOOLS workflow for the 2XND dimer dynamic network. A. The conformational ensembles were generated on a High Performance Cluster with 1440 CPU cores and 3 TB RAM. Flexibility can be represented as the root mean square deviation fit error (RMSD/ angstrom (mean $\pm$ se)) of each 4-residue averaged over the ensemble. The cytoplasmic loop (positions 38-42, 108-112) is highly flexible. **B.** Convergence of the overlap between ensemble sub-populations. Dashed line marks 99% overlap. The convergence of overlap was also examined for the monomer 2XND_A and 2XND ring ensembles. **C.** The SA has 25 representative fragments of 4 consecutive C^{α} atoms. Each fragment is associated with a letter representing a prototypical conformational state derived from an analysis of 325,923 fragments from 1830 protein domains (1). The protein sequences were encoded into a structural string of length m – 3, where m is the number of residues. Accordingly, a conformational ensemble was condensed to a list of structural strings. Local conformations of 4-residue fragments were encoded with the SA. Alpha helical backbone conformations are associated with letters W-T; beta sheet backbone conformations by letters A-G (1). The cytoplasmic loops fluctuate between alpha-helical and the more extended beta-sheet conformations. **D.** The dynamic network architecture obtained by covariance analysis of the encoded fragment motions was visualized with Cytoscape 3.0 (*http://www.cytoscape.org/*) and mapped onto the PDB structures. Bio3D (2, 3) was used for computation of the entropy and analysis of model networks, together with the igraph network library in R (*http://www.igraph.org).* The fragments constitute nodes and the correlations between them edges. Nodes coupled to the GGGG-motif node (G19 – A22 (red asterisk)) are in yellow.

Figure S2: PCA of the 2XND c_8-ring. The first three principal components (PC1 = red, PC2 = blue, PC3 = green) are plotted as a function of residue number for the eight subunits represented as discrete panels.

Figure S3: Measurement of the PC1 / PC2 motions of the assemblies: The variation in the angle between two vectors (vector 1, vector 2) in trajectory files of the 2XND ring and the isolated dimer or monomer structures (right). The vectors and planes used for the measurements are drawn in the schematics on the left (green /blue subunit C^{α} backbones, red = residues used). The vectors are formed either between the C^{α}-C^{α} atoms (bars) of two residues (example: 2XND ring V1 connects residues V5 and K294) or perpendicular (thick arrowed bars) to a plane (lines) formed by the C^{α}-C^{α} atoms of three residues (example: 2XND ring V3 is formed between residues F53, G80 and E345).

The monomer PC3 also shows a 10^{o} bending motion analogous to the PC1, but orthogonal to it. The groups were chosen based on examination of the motions captured in the movies and kymo-images.

Figure S4: Secondary structure periodicity in the co-evolution and dynamic correlation matrices. A. Left: Centrality profile correction for residual correlations: The centrality profile for the randomized 2XND library approximated an ideal random network, but with deviations at the sequence termini and adjacent to the cytoplasmic loop due to the limited number of sequences covering these regions. The randomized library profile (n = 100) was subtracted from the real profile (see Methods). Reference lines (short dashed lines) either side of the zero mean difference give a scaled estimate of one standard deviation (σ) in *E(i)* values obtained for the randomized library profile. **Right:** Auto-correlation function shows periodic peaks in the un-filtered real centrality profile due to the axial alpha-helical repeat. The profiles (Left) were filtered (4-residue running average) to remove this correlation. **B. Left:** Local dynamic correlation matrix for the isolated 2XND dimer. Matrix elements are coloured according to their nMI values. One block of the inter-subunit correlations is demarcated. The block is mirror-symmetric along the diagonal. **Right:** Auto-correlation function shows the inter-subunit dynamic couplings are also characterized by the axial alpha-helix periodicity due to the close-packing.

1. Pandini, A., A. Fornili, and J. Kleinjung. 2010. Structural alphabets derived from attractors in conformational space. BMC bioinformatics 11:97.
2. Grant, B. J., A. P. Rodrigues, K. M. ElSawy, J. A. McCammon, and L. S. Caves. 2006. Bio3d: an R package for the comparative analysis of protein structures. Bioinformatics (Oxford, England) 22:2695-2696.
3. Skjaerven, L., X. Q. Yao, G. Scarabelli, and B. J. Grant. 2014. Integrating protein structural dynamics and evolutionary analysis with Bio3D. BMC bioinformatics 15:399.

SUPPLEMENTARY MOVIES

Movie S1: 2XND Ring. PC1. En-Face View; The C^{α} backbones are colour coded (red = low, green = medium, blue = high) to indicate the root mean square fluctuation (RMSF). Residues A5 and P39 at the membrane boundary are marked by white spheres; residue G21 within the GGGG motif at the membrane mid-plane by the yellow sphere.

Movie S2: 2XND Ring. PC1.Side-On View: The C^{α} backbones are colour coded as in Movie S1. Residues A5, P39 and G21 are marked by coloured spheres as in Movie S1.

Movie S3: 2XND Ring. PC2. Side-On View: The C^{α} backbones are colour coded as in Movie S1. Residues A5, P39 and G21 are marked by coloured spheres as in Movie S1.

Movie S4: 2XND Ring. PC3. Side-On View: The C^{α} backbones are colour coded as in Movie S1. Residues A5, P39 and G21 are marked by coloured spheres as in Movie S1.

Movie S5: 2XND Monomer. PC1. Side-On View: The C^{α} backbone is colour coded as in Movie S1. Residues G19, V17 and G21 on the internal helix are marked by yellow spheres. Residues E57, G9, I31, Q44 and L69 are marked by white spheres.

Movie S6: 2XND Dimer. PC1. Side-On View: The C^{α} backbones are colour coded as in Movie S1. Residues A5, P39 and G21 are marked by coloured spheres as in Movie S1.

Movie S7: 2XND Dimer. PC1. En-Face View: The C^{α} backbones are colour coded as in Movie S1. Residues A5, P39 and G21 are marked by coloured spheres as in Movie S1.

Movie S8: 2XND Monomer. PC2. Side-On View: The C^{α} backbone is colour coded as in Movie S1. Residues G19, V17 G21, E57, G9, I31, Q44 and L69 are marked by coloured spheres as in Movie S6.

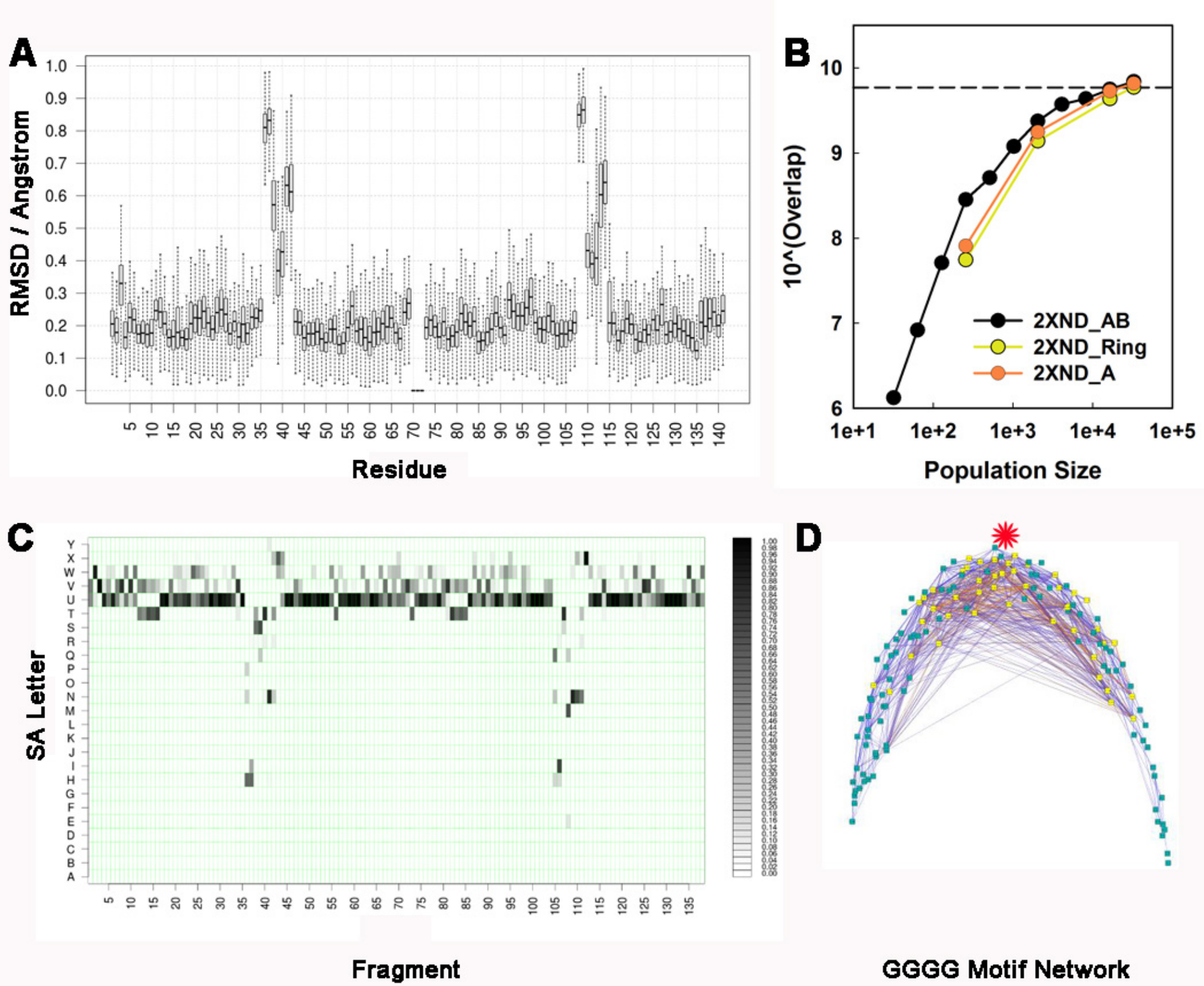
A
RMSD / Angstrom
Residue
B
10^(Overlap)
Population Size
2XND_AB
2XND_Ring
2XND_A
C
SA Letter
Fragment
D
GGGG Motif Network

Figure S1

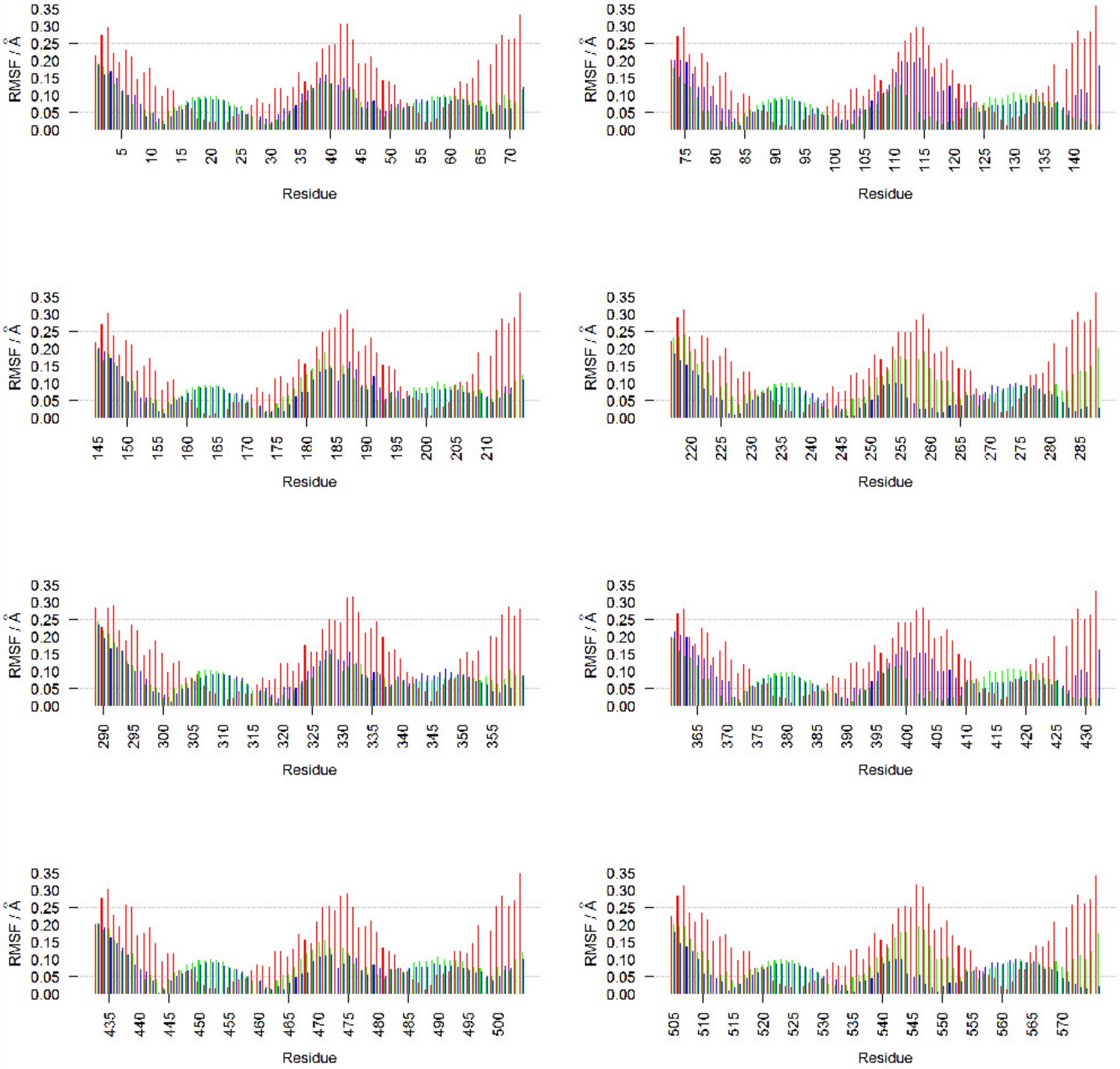
RMSF / Å
0.35
0.30
0.25
0.20
0.15
0.10
0.05
0.00
5 10 15 20 25 30 35 40 45 50 55 60 65 70
75 80 85 90 95 100 105 110 115 120 125 130 135 140
145 150 155 160 165 170 175 180 185 190 195 200 205 210
220 225 230 235 240 245 250 255 260 265 270 275 280 285
290 295 300 305 310 315 320 325 330 335 340 345 350 355
365 370 375 380 385 390 395 400 405 410 415 420 425 430
435 440 445 450 455 460 465 470 475 480 485 490 495 500
505 510 515 520 525 530 535 540 545 550 555 560 565 570
Residue

Figure S2

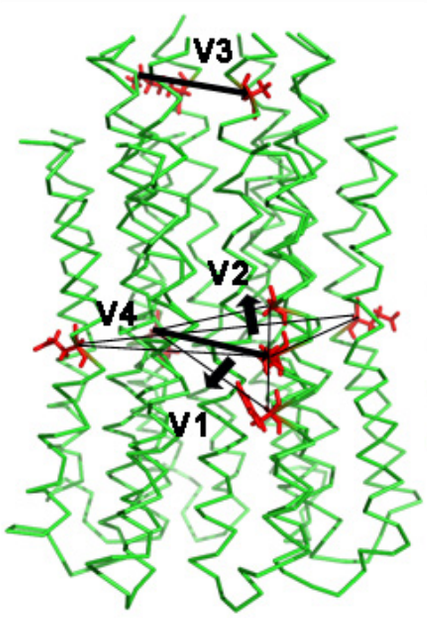

2XND_Ring

MOTION	VECTOR_1	VECTOR_2	VALUE_PC1	VALUE_PC2
Radial Dispersion	V! (F53-G60-E345)	V3 (V5-V293)	13.7°	1.9°
Radial Dispersion	V1 (F53-G60-E345)	V4 (E57-E345)	2.4°	0.16°
Axial Dispersion	V2 (E241-E345-E489)	V3 (V5-V293)	1.35°	5.47°
Axial Dispersion	V2 (E241-E345-E489)	V4 (E57-E345)	0.02°	0.11°

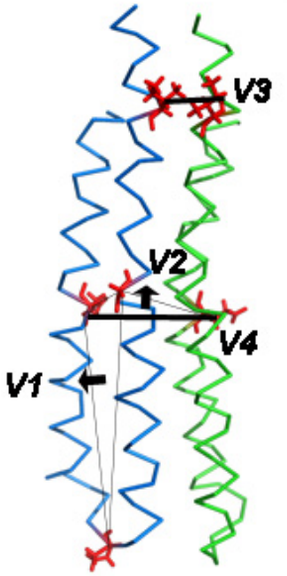

2XND_Dimer

MOTION	VECTOR_1	VECTOR_2	VALUE_PC1	VALUE_PC2
Radial Dispersion	V1 (G19-E57-P39)	V3 (I8-I80)	25.3°	1.1°
Radial Dispersion	V1 (G19-E57-P39)	V4 (E57-E129)	1.5°	4.9°
Axial Dispersion	V2 (G19-E57-E129)	V3 (I8-I80)	20.0°	1.1°

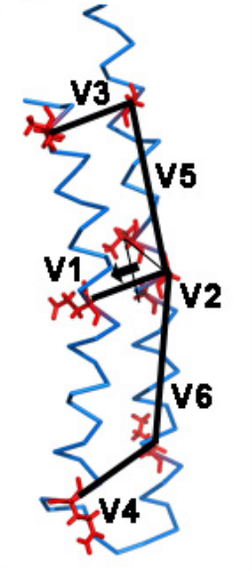

2XND_Monomer

MOTION	VECTOR_1	VECTOR_2	VALUE_PC1	VALUE_PC2
Radial Dispersion	V1 (G19-V17-G21)	V2 (G19-E57)	2.94°	1.84°
Radial Dispersion	V1 (G19-V17-G21)	V3 (G9-L69)	1.9°	15.06°
Radial Dispersion	V1 (G19-V17-G21)	V4 (I31-Q44)	4.58°	14.12°
Axial Dispersion	V5 (G19-G9)	V6 (G19-I31)	10.09°	0.67°

Figure S3

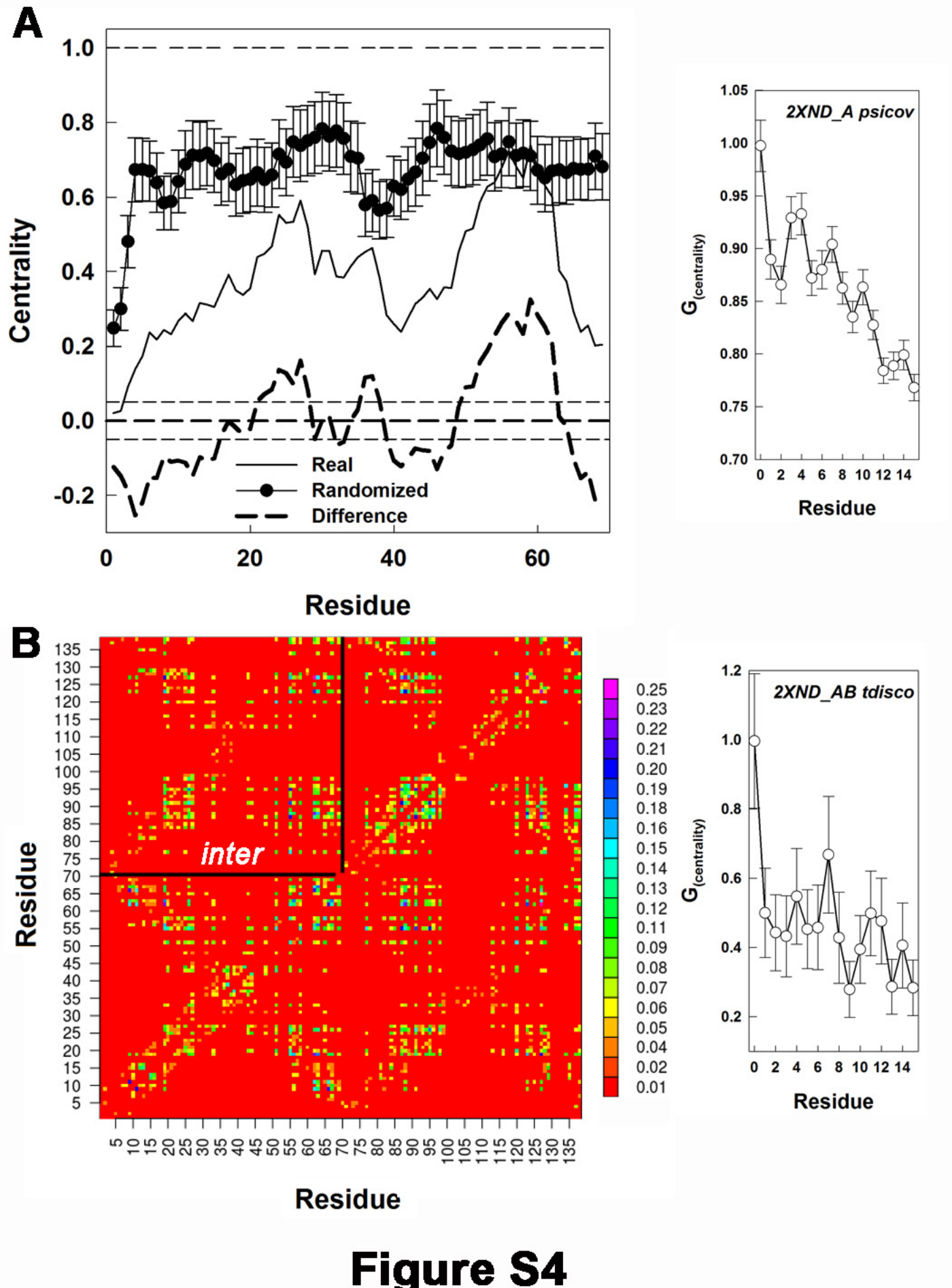
A
Centrality
Residue
Real
Randomized
Difference
2XND_A psicov
G(centrality)
Residue
B
Residue
inter
Residue
2XND_AB tdisco
G(centrality)
Residue

Figure S4